*Thermochimica Acta*
Elsevier Publishing Company, Amsterdam
Printed in Belgium

# THERMOGRAVIMETRY OF THERMALLY STABLE AROMATIC AND HETEROCYCLIC POLYMERS*

R. W. FARMER

*Air Force Materials Laboratory, Wright-Patterson AFB, Ohio 45433 (U. S. A.)*

(Received February 11th, 1972)

## ABSTRACT

Thermally stable polymers were studied using thermogravimetry (TG) to 1400°C in helium. The heterocyclics were a polybenzimidazole and a polyimide. The aromatics consisted of two phenol formaldehydes, a phenylphenol phenol formaldehyde, and two polyphenylenes.

Computer code analysis provided rate parameters for an Arrhenius type correlation. The rate parameters represented well the TG run.

Overall pyrolysis mechanisms were examined in terms of rate parameters and computer code curves, which normalized out the polymer char yield and reinforcing fiber content.

Standardization was emphasized to provide quality TG data and accurate parameters relatively free from procedural variables of polymer synthesis, degree of cure, sample preparation, thermobalance operation, data analysis, and pyrolysis beyond 1000°C.

## SYMBOLS

| | |
|---|---|
| $A$ | kinetic parameter, min$^{-1}$ |
| $A'$ | kinetic parameter, min$^{-1}$ |
| e | logarithmic base, dimensionless |
| $E$ | kinetic parameter, kcal/g-mole |
| exp | exponential to be base e, dimensionless |
| f | function |
| $k$ | kinetic parameter, min$^{-1}$ |
| $K$ | integral parameter, dimensionless |
| ln ( ) | logarithm to the base e, dimensionless |
| $\log_{10}$ ( ) | logarithm to the base 10, dimensionless |
| $m$ | series term, dimensionless |
| $n$ | kinetic parameter, dimensionless |
| p($X$) | functional equation, dimensionless |
| $r$ | relative error, dimensionless |

---

*Presented before the Third Annual Meeting of the North American Thermal Analysis Society in Waco, Texas, on February 7–8, 1972.

| | |
|---|---|
| $R$ | gas constant, kcal/g-mole/°K |
| $t$ | time, min |
| $T$ | temperature in degrees absolute*, °K |
| $w$ | residue-free basis weight fraction, dimensionless |
| $w_{0}$ | sample weight fraction, dimensionless |
| $w_{0i}$ | initial sample weight fraction, dimensionless |
| $w_r$ | residual sample weight fraction, dimensionless |
| $X$ | $E/RT$, dimensionless |
| $(\dot{\ })$ | $d(\ )/dt^*$, $\min^{-1}$ |
| $(\dot{\ })_T$ | $d(\ )/dT^*$, $°K^{-1}$ |
| $m$ | maximum rate of weight loss, subscript |
| 1, 2 | singular case, subscript |

## INTRODUCTION

Many aromatic and heterocyclic polymers, with such structures as idealized by Fig. 1, possess remarkable levels of thermal stability. Non-standard procedures

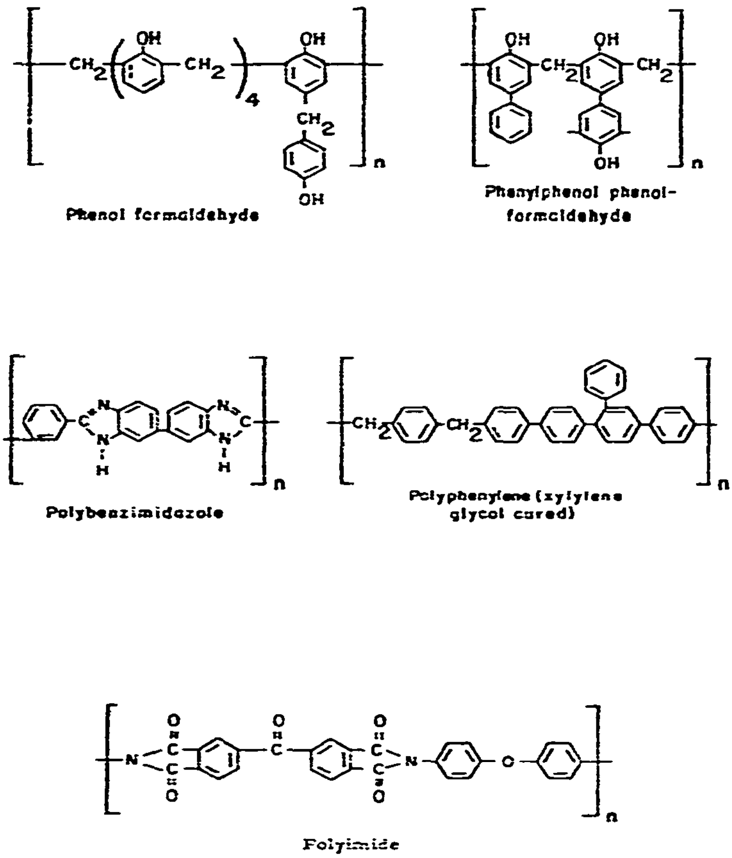
Phenol formaldehyde

Phenylphenol phenol-formaldehyde

Polybenzimidazole

Polyphenylene (xylylene glycol cured)

Polyimide

Fig. 1. Representative structural formulas of aromatic and heterocyclic polymers.

---

*Different units for a symbol are noted with that symbol.

used in early thermal analysis, further complicated by synthesis and analysis variables, has restricted the evaluation of kinetic rate parameters and thermal effects. In the present work, an attempt was made to realistically portray the thermal stability of representative polymers on comparative scales.

## EXPERIMENTAL

### *Recording thermobalance*

The modified Aminco Thermo-Grav recording thermobalance is illustrated by Fig. 2. A weight–temperature–time curve was automatically plotted by an X–$Y^1$–$Y^2$ recorder. During the run a change in sample weight caused two precision springs to

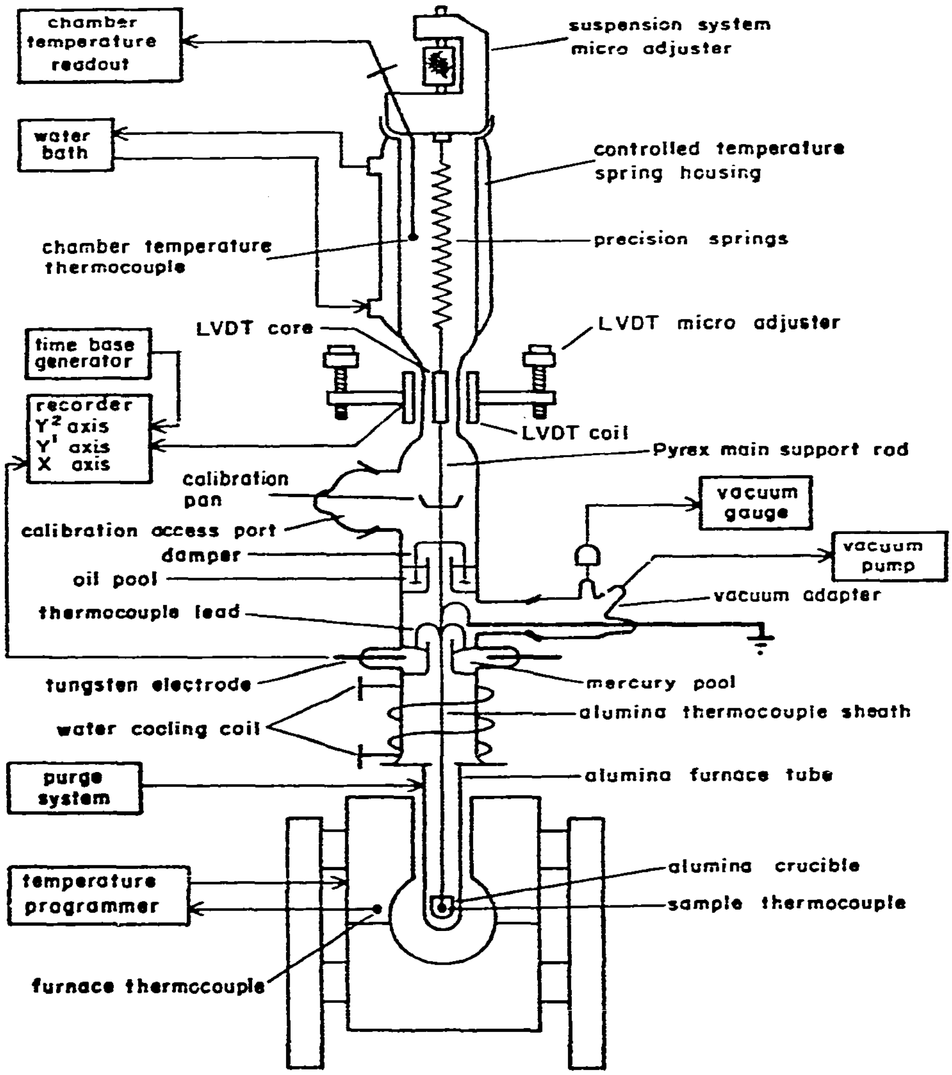

Fig. 2. Diagram of the recording thermobalance.

move. A linear variable differential transformer (LVDT) response voltage drove one recorder pen. A platinum-platinum/13% rhodium-platinum (ground) thermocouple produced the e.m.f. to move the X-axis carriage. Run time was plotted by the $Y^2$ pen by means of a synchronous time-base generator.

The Pyrex support rod was joined to the springs just below the housing. The rod held an LVDT core, weight pan, and an oil dashpot ring. The crucible, thermocouple, and alumina sheath hung from the rod into the furnace.

The sample thermocouple signal was grounded and filtered to shield against noise pickup at high temperatures. The feedthroughs (fine tungsten-wire lead–mercury pool–tungsten electrode) had little mechanical effect upon spring linearity.

The original tubular crucible (McDanel Refractory Porcelain Company body AP35 recrystallized alumina) had the dimensions 1/4 in. inside diameter, 3/8 in. outside diameter, and 1 in. length. The crucible was ground to give two lobes and a remaining 1/2 in. of outside length. For support, an alumina pin was placed through a hole in each of the opposing lobes and a hole in the sheath.

The spherical furnace (Tem-Press Research, Inc., Model SQ-IC-4) was controlled by an SCR power programmer (F & M Model 240M). A strip chart recorder (Leeds & Northrup) plotted a temperature–time history for the Pt–Pt/10% Rh control thermocouple. The 1 in. outside diameter by 9.5 in. length furnace tube was made of alumina (McDanel body AP35).

In addition to a controlled temperature spring housing, there were water cooling provisions for the furnace periphery and the three mercury pools.

*Standard run*

A −325 sieve, dried powder was run at 8.5°C/min to 1400°C in a helium purge flowing at an inlet rate of 1 liter/min.

The sample and residue were weighed with an analytical balance. The sample weights were 40 mg for a phenol formaldehyde molding and 80 mg for all other materials.

Although no inordinately special techniques were used, such as for precision sample packing, all procedures were well-practiced and were followed consistently.

The calibrated $X$–$Y^1$–$Y^2$ recorder ranges were 0–20 mg/5 in., 0–16 mV/20 in., and 0–200 min/5 in., respectively. This weight ordinate gave either a 50% or a 25% total span for the two sample weights. The abscissa was convertible to a non-linear, reference temperature span of 0–1402°C. The reciprocal slope of the run time curve was the heating rate.

Two recorder sweeps were made to improve precision. To do this, the carriage was manually shifted back to zero after 10 in. of travel (to 806°C) to give 20 in. of chart (to 1402°C).

The thermobalance atmosphere was purified by three consecutive evacuation and helium fill cycles. The helium purge resulted from a final internal pressurization to slightly above atmospheric pressure.

### *Materials*

The structure of an aromatic or heterocyclic polymer is dependent upon numerous variables of synthesis, cure, etc. In some cases, a suitable bulk polymer is not easily made or may have no known preparation. Commercial polymers, as used to prepare well-cured carbon and graphite cloth reinforced composites, helped reduce the effects of these structural variables.

The polymers consisted of two phenol formaldehydes (American Reinforced Plastics Company CTL-91LD and Monsanto Chemical Corporation RI4009), a polybenzimidazole (Whittaker Corporation Imidite 2803), two polyphenylenes (Hughes Aircraft Company Abchar 412 and 413), a phenylphenol phenol formaldehyde (Hughes Aircraft Company), and a polyimide (Monsanto Chemical Company Skybond 700).

The carbon cloth (CCA-1) was described by the source (H. I. Thompson Fiberglas Company) as a fully amorphous material with a 97% carbon content. The graphite cloth (G1550) was further reported to be a more crystalline, high-purity form with a carbon content of 99.6% and an ash content of less than 0.1%.

### *Preparation of materials*

*Composites.* — As shown by Table I, the carbon cloth and the graphite cloth were initially air oven dried for 1–2 h at about 95–115 °C. Weight loss ranged up to 10% for the carbon cloth.

The first step in using the "as received" resin was usually dilution for a reduced solids content and good cloth coating. In addition to brush, dip, and spatula coating methods, a laboratory tower coater was used for one large batch.

An initial air drying of the coated cloth was followed by up to three resin staging cycles for up to one hour at temperatures up to 120 °C.

After shaping the staged prepreg plies, the necessary number was transferred to a molding fixture. The material was compression molded up to maximum conditions of 10,000 p.s.i., 370 °C, or 3 h.

The molded composites were postcured at various times at temperatures up to 455 °C. Three postcures were made under an inert gas purge to avoid oxidation or other difficulties. To further avoid possible blistering, blow-up, or related effects, 4 of the 8 composites were roughly cut into the final shape before postcuring.

All resin content calculations summarized by Table I were based upon the initial dry reinforcement weight. The change in resin content from air-dried, coated material to postcured composite varied markedly with resin type. The maximum change was 22% for polyimide–graphite cloth.

*Molding.* — The phenol formaldehyde molding was prepared from a novolac resin (Monsanto Chemical Company RI4009). The molding was made in a small stainless steel jig. The loaded jig was processed at 320 p.s.i. for 30 min at 92 °C with a gradual change over a 15-min period to 160 °C, which was held for 30 min.

The postcure temperatures of 150 °C and 178 °C were for 24 h each with the jig at a pressure of 320 p.s.i.

TABLE I

EXPERIMENTAL MATERIALS

| *A. Sample description* | *Carbon cloth materials* | | | | *Graphite cloth materials* | | | |
|---|---|---|---|---|---|---|---|---|
| | *Phenol formaldehyde* | *Polybenz-imidazole* | *Polyphenylene* | *Polyimide* | *Phenol formaldehyde* | *Phenylphenol phenol formaldehyde* | *Polyphenylene* | *Polyimide* |
| *B. Prepreg processing* | | | | | | | | |
| Reinforcement drying time (h), at each temp (°C) | 2, 116 | | 2, 116 | 1, 93 | 2, 116 | 2, 116 | 2, 116 | 2, 116 |
| Resin dilution | | | | | | | | |
| Agent | acetone | | | | acetone | | acetone | acetone |
| Resin/Agent ratio | 1/0.5 | | | | 1/0.7 | | 1/0.7 | 1/0.4 |
| Prepreg | | | | | | | | |
| Coating method | brush | | dip | spatula | lab coater[d] | dip | spatula | spatula |
| Staging time (h), at each temperature (°C) for cycle 1[a] | 1, RT | | 0.3, RT | 1, RT | ?, 116 | 0.5, RT | 0.3, RT | 0.4, RT |
| 2 | 1, 71 | | 0.3, 71 | 0.5, 121 | | 1, 71 | 0.3, 71 | 1, 93 |
| 3 | 0.3, 107 | | | | | | | |
| *C. Processing* | | | | | | | | |
| Cure | | | | | | | | |
| Contact time (min) | 5 | 20 | 0 | 10 | 5 | 0 | 0 | 0 |
| Pressure, p.s.i. | 300 | 500 | 1000 | 500 | 10000 | 10000 | 10000 | 10000 |
| Time (h), at each temp (°C) | 3, 149 | 1.5, 371 | 2, 204 | 2, 316 | 2, 149 | 2, 216 | 2, 149 | 2, 316 |
| Postcure | | | | | | | | |
| Cycle code[b] | B | K-3 | M | R | B | I-2 | B | R |
| Machined ?[c] | yes | yes | no | yes | no | no | no | yes |
| Number of parts[c] | 30 | ? | | 4 | | | | 2 |

*D. Postcured laminate*

| | | | | | | | | |
|---|---|---|---|---|---|---|---|---|
| Barcol hardness | 70 | ,0 | 58 | 45 | 38 | 35 | 52 | 35 |
| Density (g/cc) | 1.38 | 1.34 | 1.33 | 1.22 | 1.31 | 1.25 | 1.34 | 1.21 |
| Number of plies[d] | 52 | 60 | 48 | 40 | 207 | 182 | 200 | 185 |
| Overall dimensions (in.)[d] | 16.75 × 18 × 0.5 | 7 × 8 × 0.5 | 3.5 × 0.585 | 3 × 3 × 0.5 | 1.68 × 2.33 | 1.68 × 2.22 | 1.68 × 2.24 | 3 × 5 |
| Resin content (percent)[e] | 37.9 | 37.4 | 34.4 | 42.0 | 36.3 | 36.6 | 37.2 | 23.4 |
| Specimen type | hot gas flow | laminate | pellet | pellet | pipe | pipe | pipe | pipe |
| Void content (percent)[e] | 22.3 | 29.7 | 26.3 | | | | | |

*E. Resin content and weight history*[h]

| Code | CTL-91LD | | Imidite 2803 | | Abchar 413 | | Skybond 700 | | CTL-91LD | | Abchar 412 | | None | | Skybond 700 | |
|---|---|---|---|---|---|---|---|---|---|---|---|---|---|---|---|---|
| Item | Grams | %RC | Grams | %RC | Grams | %RC | Grams | %RC | Grams | %RC | Grams | %RC | Grams | %RC | Grams | %RC |
| Reinforcement | 2769.9 | 0 | | | 144.0 | 0 | 78 | 0 | 1348.2 | 0 | 178.1 | 0 | 278.9 | 0 | 484.0 | 0 |
| Staging cycle 1 | 5211.5 | 45.8 | | | 253.0 | 43.1 | | | 2185.2 | 38.3 | 342.5 | 48.0 | | | | |
| 2 | 4834.5 | 42.7 | | | 242.0 | 40.5 | 188.5 | 58.6 | | | 296.6 | 40.0 | 481.2 | 42.0 | 1068.0[i] | 54.7[i] |
| 3 | 4669.5 | 40.7 | | | | | | | | | | | 457.2 | 39.0 | 1007.8 | 52.0 |
| Molded laminate | | | | | | | | | | | | | | | | |
| Prepreg | 4642.0 | 40.7 | 884.1 | 43.2 | 134.4 | 40.5 | 175.0 | 58.6 | 116.6 | 38.3 | 106.0 | 40.0 | 112.5 | 39.0 | 821.0 | 52.0 |
| Laminate | 4590.0 | 40.0 | 810.0 | 38.0 | 128.3 | 37.6 | 130.0 | 44.3 | 116.1 | 39.2 | 102.0 | 37.6 | 112.0 | 38.8 | 587.5 | 32.9 |
| Machined parts | 4148.5 | 40.0 | 763.0 | 38.0 | | | 126.0 | 44.3 | | | | | | | 571.1 | 32.9 |
| Postcured laminate (or parts) | 4008.0 | 37.9 | 756.0 | 37.4 | 122.0 | 34.4 | 121.0 | 42.0 | 110.9 | 36.3 | 100.3 | 36.6 | 109.2 | 37.2 | 566.5 | 32.4 |

---

[a] RT = air dried at room temperature. [b] Postcure cycle details as follows: B; 18 h at 135°, 72 h from 135° to 204°, 4 h at 204°, 7 h cooling to below 93°C I-2; 18 h at 135°, 92 h from 135° to 288°, cooled to below 93°C. Postcured in a helium atmosphere. K-3; 26 h from room temperature to 316°, 24 h at 316°, 10 h from 316° to 343°, 24 h at 343°, 10 h from 343° to 371°, 24 h at 371°, 10 h from 371° to 399°, 6 h at 399°, 10 h from 399° to 427°, 6 h at 427°, 10 h from 427° to 454°, 6 h at 464°, 10 h cooling to below 93°C. Postcured in an argon atmosphere. M; 18 h at 135°, 108 h from 135° to 288°, 6 h at 288°, 7 h cooling to below 93°C. Postcured in an argon atmosphere. R; 24 h at 190°, 24 h at 224°, 24 h at 246°, 24 h at 301°, 7 h cooling to below 93°C, 6 h between each temperature level. [c] Some laminates were cut into small parts to reduce the possibility of blowup during postcure. [d] Number of cloth plies in the thickness direction prior to part, pellet, or pipe machining. [e] Resin content by weight percent of resin. Void content by volume percent of voids in the resin. Resin content of postcured laminate assumed unchanged during machining; resin content of final prepreg assumed unchanged until molding. [f] Prepreg was provided by the source. The prepreg resin content was by extraction. [g] The cloth was coated and staged in a laboratory coater. The tower temperature was 116°C and the cloth speeds were 12 in./min and 16 in./min for runs 1 and 2, respectively. 207 each plies of runs 1 and 2 were randomized; the mixture was divided into equal parts for molding 2 laminates. [h] Blank spaces designate data not determined. [i] Vacuum dried at room temperature for 4 h without weight loss.

### *Preparation of sample*

The lathe method essentially consisted of the slow machining of bulk stock using a tungsten dicarbide-tipped, "low bite" cutter. To avoid postcure, previous machining, or like defects, a surface layer was first removed from the test composite. To deface, a vigorous initial sanding (240-grit or 400-grit silicon carbide paper) was followed by lathe surfacing. After up to four coarse passes, the stock was again cleaned thoroughly. The cutting speed and depth-of-cut were then changed for powder production.

A constant lathe chuck speed of 52 r.p.m. was used with cut depths ranging from 0.001–0.003 in. to 0.0005–0.001 in. for surfacing and sampling, respectively. The traversal speed of the tool was generally 0.0027 in./rev. (or 128 turns/in.).

The lathe method gave a high yield of −325 sieve powder. The powder fraction was microscopically inspected for quality indices such as configuration, grain size, gross distribution, etc., before and after sieving.

All sieved powders were "dried" in a small vacuum oven for 50 min at 125°C and about 18 in. of mercury pressure. Without taking extreme precautions, every practical effort was made to minimize atmospheric exposure before or after a thermogravimetric run.

## EMPIRICAL KINETICS

### *Residue-free basis weight*

In order to examine kinetic and thermal stability in terms of polymer composition, it was convenient to define a weight that normalized out the char yield and cloth stable residue at 1400°C. This value $w$ defined by

$$w = (w_0 - w_r)/(w_{0i} - w_r) \qquad (1)$$

was termed a "residue-free" weight fraction.

The material available for pyrolysis was the initial-weight to stable-weight fraction difference, $(w_{0i} - w_r)$. Effectively, for a residue-free weight basis the curve was adjusted to a new scale of unity-to-zero $w$ using this term.

### *Kinetic analysis*

The isothermal relationships

$$-\dot{w} = kw^n \qquad (2)$$

$$k = A \exp -X \qquad (3)$$

were the basis for the kinetic analysis.

An equivalent constant heating rate relation for Eqns. (2) and (3) was

$$-\dot{w}_T = (w^n A/\dot{T}) \exp -X \qquad (4)$$

and was rearranged as

$$K = -\int_{1}^{w} w^{-n}\,\mathrm{d}w = (A/\dot{T})\int_{0}^{T} \mathrm{e}^{-X}\,\mathrm{d}T \tag{5), (6}$$

where $K$ was a convenient functional symbol.

Integration of Eq. (6) by parts in two different ways gave

$$K = (AE/R\dot{T})\,\mathrm{p}(X) \tag{7}$$

$$\mathrm{p}(X) = X^{-1}\,\mathrm{e}^{-X} - \int_{X}^{\infty} X^{-1}\,\mathrm{e}^{-X}\,\mathrm{d}X \tag{8}$$

$$K = (AE/R\dot{T})\left[1 - \sum_{m}(-1)^{m+1}\,X^{-m}\,(m+1)!\right]X^{-2}\,\mathrm{e}^{-X} \tag{9}$$

For $m = 0$, a relative error $r$ was defined for the ratio of Eqns. (7) and (9) as

$$r = X^{2}\,\mathrm{e}^{X}\,\mathrm{p}(X) \tag{10}$$

and gave an additional useful expression for $K$

$$K = r(AE/R\dot{T})\,X^{-2}\,\mathrm{e}^{-X} \tag{11}$$

One computer code, called MAXRAX, calculated an $(n, A, E)$ set from maximum rate of weight loss experimental data. Essentially, the four relations

$$A = (w^{1-n}\,\dot{T}X/nT)\,\mathrm{e}^{X} \tag{12}$$

$$E = -\dot{w}_{T}nRT^{2}/w \tag{13}$$

$$n = \{\ln[r(n^{-1}-1)+1]\}/\ln w + 1 \tag{14}$$

$$r = X^{2}\,\mathrm{e}^{X}\,\mathrm{p}(X) \tag{15}$$

were solved by an iterative procedure further using the tabulated tables

$$r = \mathrm{f}_{1}(X) \tag{16}$$

$$w = \mathrm{f}_{2}(n, r) \tag{17}$$

MAXRAX resulted from a maximum rate of weight loss solution of Eqns. (2) and (3), namely, Eqn. (13). The other relations for $A$ and $n$ came from a comparison of Eqn. (13) with Eqns. (2), (3), and (11).

The second computer code TRIM calculated $A$ and $E$ from weight fractions as a function of temperature. This integral method solved

$$\log_{10}(K/T^{2}) = (-E/R\ln 10)(1/T) + \log_{10} r(AR/E\dot{T}) \tag{18}$$

which was derived from Eqn. (11). The terms $(-E/R\ln 10)$ and $\log_{10} r(AR/E\dot{T})$ were made equal to a slope and intercept, respectively, for this nearly linear equation. $A$ and $E$ were estimated by the standard method of least squares.

In operation, TRIM first converted the observed weight fraction $w_0$ to a residue-free basis value by means of Eqn. (1). A $K$ value was ten calculated

$$K = -\ln w \tag{19}$$

for $n = 1$, and

$$K = (w^{1-n} - 1)/(n-1) \tag{20}$$

for $n \neq 1$

for the MAXRAX-$n$ or a selected value of $n$. Eqns. (19) and (20) were the solution of Eqn. (5).

TRIM incremental temperatures corresponded to 0.1-in. divisions of chart paper. As for conventional practice, small rate of weight loss points at the start and first sweep end of the curve were discarded. The useful "q temperature span" was estimated for each case (up to 99 points to 806°C).

The use of the standard method of least squares was an approximation for TRIM. All the terms in Eqn. (18) were interdependent, the experimental precision was variable, and the MAXRAX term, $r$, slowly decreased with increasing temperature (no more than ±4% maximum change within the q temperature span). Therefore, a second parameter $A'$ was calculated using maximum rate of weight loss data

$$A' = -\dot{w}_T w^{-n} \dot{T} e^X \tag{21}$$

to compare with $A$. Eqn. (21) was derived from Eqn. (4).

PAR 3 was a computer code for graphical construction of a curve from an ($n$, $A$, $E$) set. Eqn. (7) was solved using a p($X$) table. A $w$ value, from the converse of Eqn. (19) or (20), became a $w_0$ using the converse of Eqn. (1). Up to 199 weight fractions for 0.1-in. increments of chart from 14.4°C were graphed by an X-Y plotter.

W-DΦ was a simple computer code for the calculation of a $w$ value from a $w_0$ input using Eqn. (1). The two temperature options were for either equal incremental spacing of chart paper or individual numerical prefixes. The former option of 0.1-in. increments of chart paper corresponding to the TRIM $w_0 - T$ inputs was generally used for this work. Since W-DΦ was not combined with PAR 3, it was necessary to manually replot $w$ as a function of displacement. The individual points were then connected by a smooth curve.

## RESULTS AND DISCUSSION

### *Experimental curves*

The curves for the carbon cloth and graphite cloth composites were sketched together for comparative purposes (Figs. 3 and 4). The curves for the phenol formaldehyde and phenylphenol phenol formaldehyde materials resembled a somewhat elongated arc tangent function. The polyimide and polyphenylene curves were more sinusoidal in shape. The heterocyclic polybenzimidazole gave a relatively complex curve.

A subjective order of thermal stability, or highest-weight retention at constant temperature, was polybenzimidazole > polyphenylene > polyimide > phenylphenol phenol formaldehyde and phenol formaldehyde for the five polymer classes.

With the exception of the polyimide, the nominal resin contents of 34.4–37.9% for the carbon cloth materials were sufficiently similar for inter-comparison of polymer

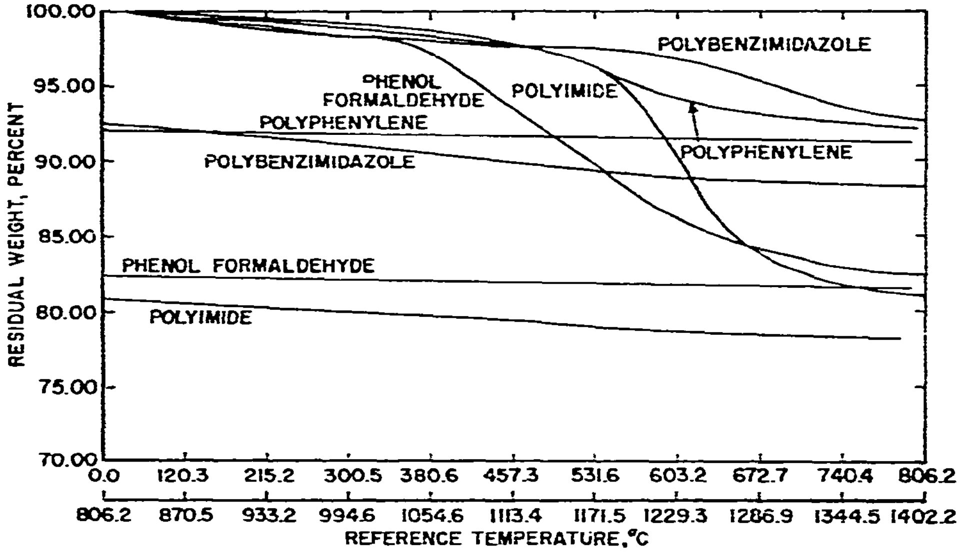

Fig. 3. Plot of residual weight *vs.* reference temperature for the polymer–carbon cloth composites.

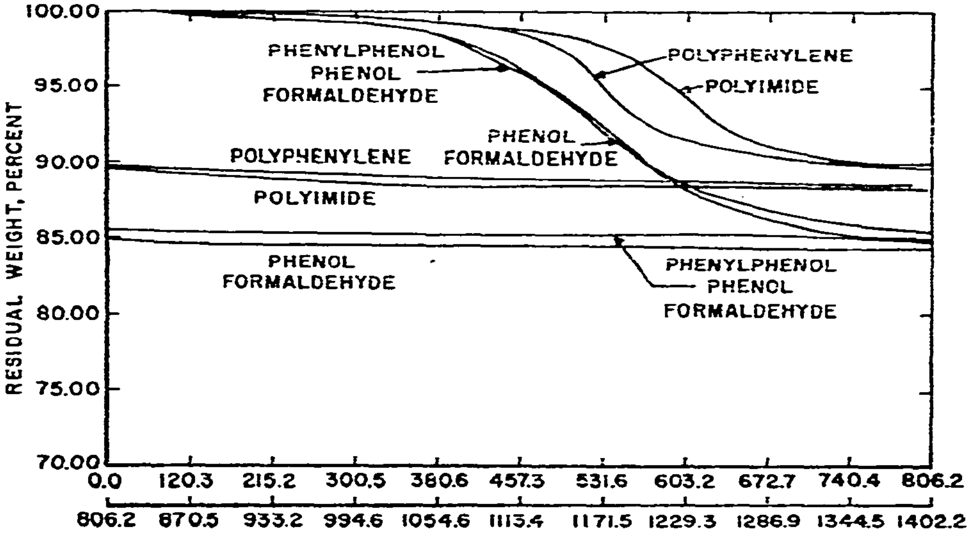

Fig. 4. Plot of residual weight *vs.* reference temperature for the polymer–graphite cloth composites.

effects alone. The high resin content of 42.0% for the polyimide explained the low apparent residual weight at 1400°C.

All carbon cloth materials were influenced by carbon cloth pyrolysis, which amounted to 87.4% residual weight at 1400°C for a cloth powder run.

The range of resin contents for the graphite cloth materials was 32.4–37.2%.

The graphite cloth constituent was relatively stable in the amount of 98.7% residual weight for a separate powder run.

A suitable polybenzimidazole–graphite cloth composite could not be made. Similarly, the phenylphenol phenol formaldehyde polymer was only available with a graphite cloth reinforcement. In addition, the two polyphenylene polymers were different with respect to curing mechanism and pre-polymer molecular weight.

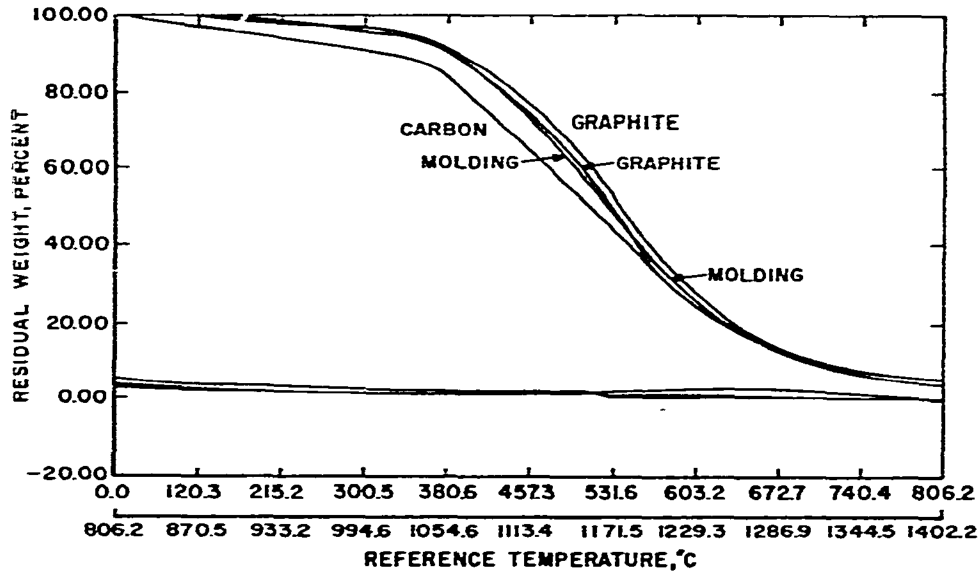

Fig. 5. Residue-free basis curves for the phenol formaldehyde resin materials.

*Residue-free basis curves*

Using the computer code W-D$\Phi$, the experimental curves were normalized to be independent of residual weight, or char yield, of pyrolyzed cloth and resin. The re-plotted curves gave information on relative thermal stability in terms of the pyrolyzable portion of the polymer.

Residue-free basis curves for the three phenol formaldehyde composites agreed well with each other and that of the pure phenol formaldehyde molding (Fig. 5).

There was an abnormal low-temperature weight loss regime and complex two-step pyrolysis for the phenol formaldehyde–carbon cloth material. This result was tentatively attributed to cloth pyrolysis and possible moisture loss at the lowest temperatures.

There was also an early weight loss for the polyphenylene–carbon cloth com-

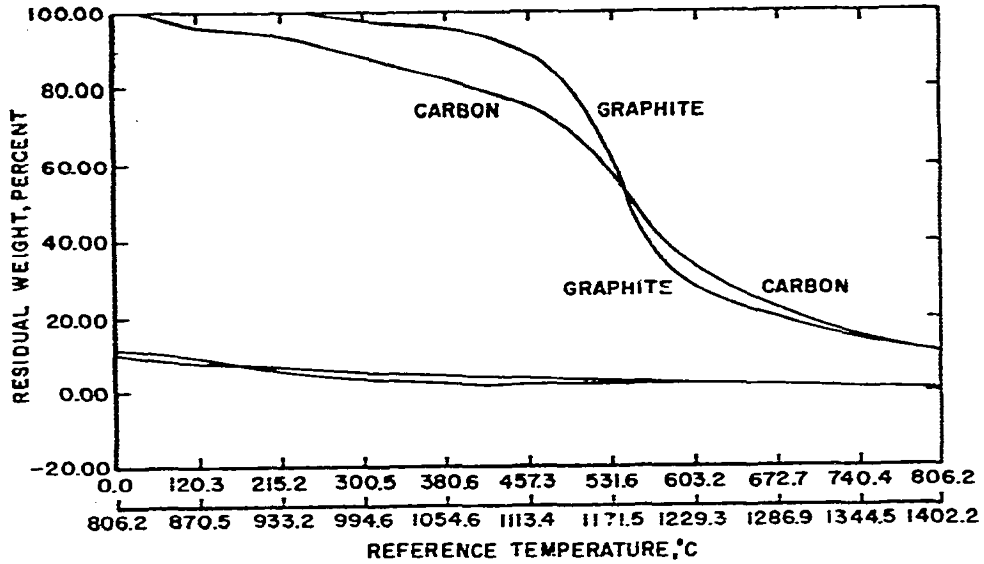

Fig. 6. Residue-free basis curves for the polyphenylene resin materials.

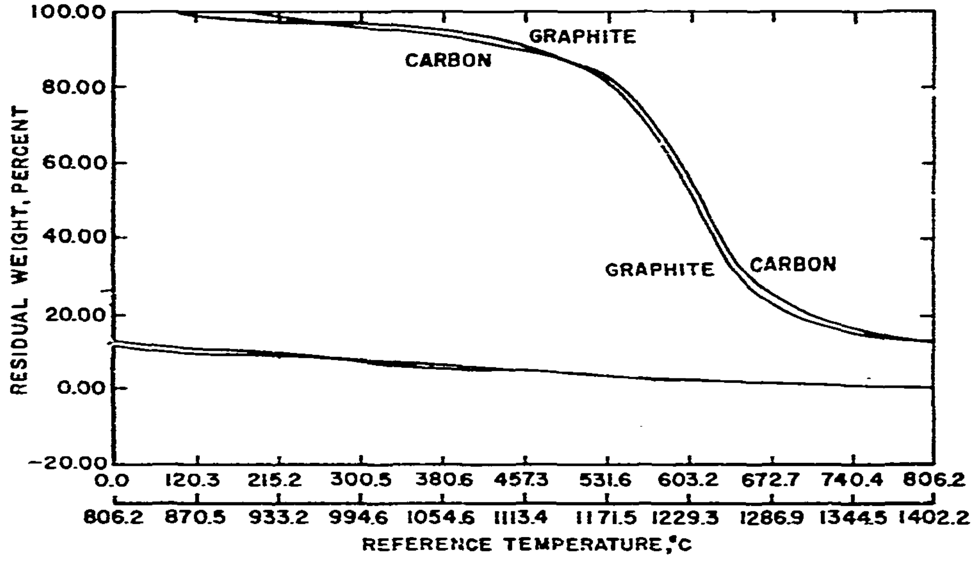

Fig. 7. Residue-free basis curves for the polyimide resin materials.

posite (Fig. 6). Although the graphite cloth material showed considerably higher stability up to about 550 °C, both samples were nearly identical at higher temperatures.

The residue-free basis curves for the polyimide resin materials are shown in Fig. 7.

*Kinetic analysis*

MAXRAX was a computer code for the computation of kinetic parameters from maximum rate of weight loss data. The nominal ranges for the carbon cloth materials were $n = 1.0\text{–}1.6$, $A = 1.7 \times 10^1\text{–}6.2 \times 10^7$, $E = 9\text{–}34$. The nominal ranges for the graphite cloth materials were $n = 1.0\text{–}3.8$, $A = 2.0 \times 10^3\text{–}5.3 \times 10^{13}$, $E = 16\text{–}52$ (Tables II and III).

TABLE II

MAXRAX AND TRIM EMPIRICAL KINETIC PARAMETERS: CARBON CLOTH MATERIALS[a]

| *Case* | *Phenol formaldehyde* | | | | *Polybenzimidazole* | | | |
|---|---|---|---|---|---|---|---|---|
| | *(MAXRAX)* | *(TRIM)* | *(TRIM)* | *(TRIM)* | *(MAXRAX)* | *(TRIM)* | *(TRIM)* | *(TRIM)* |
| $n$ | 1.01943 | 1 | 1.01943 | 2 | 1.57844 | 1 | 1.57844 | 2 |
| $A$ (min$^{-1}$) | 16.8506 | 2.56923 | 2.77266 | 232.299 | 28.9924 | 0.990225 | 4.55574 | 14.8315 |
| $A'$ (min$^{-1}$) | | 4.44641 | 4.75782 | 253.326 | | 1.68644 | 7.03150 | 21.5533 |
| $E$ (kcal/mole) | 9.06708 | 6.62627 | 6.70941 | 11.7983 | 12.2609 | 7.15963 | 9.23947 | 10.9080 |
| q span (°C) | | 325–800 | 325–800 | 325–800 | | 603–800 | 603–800 | 603–800 |
| $r_m$ | 0.782113 | | | | 0.794974 | | | |
| $\dot{T}$ (°C/min) | 8.28 | | | | 8.28 | | | |
| $T_m$ (°C) | 532 | | | | 693 | | | |
| $\dot{T}_m$ (°C/min) | 10.22 | | | | 9.69 | | | |
| $T_r$ (°C) | 1400 | | | | 1400 | | | |
| $w_m$ | 0.4455 | | | | 0.5510 | | | |
| $w_r$ | 0.816 | | | | 0.883 | | | |
| $-\dot{w}_{T_m}$ (°C)$^{-1}$ | −0.003076 | | | | −0.002305 | | | |

| *Case* | *Polyphenylene* | | | | *Polyimide* | | | |
|---|---|---|---|---|---|---|---|---|
| | *(MAXRAX)* | *(TRIM)* | *(TRIM)* | *(TRIM)* | *(MAXRAX)* | *(TRIM)* | *(TRIM)* | *(TRIM)* |
| $n$ | 1.50455 | 1 | 1.50455 | 2 | 2.10816 | 1 | 2.10816 | 2 |
| $A$ (min$^{-1}$) | 1698.47 | 0.636629 | 3.09617 | 16.9989 | $6.28046 \times 10^7$ | 6.16608 | 149.572 | 106.417 |
| $A'$ (min$^{-1}$) | | 1.95239 | 7.69345 | 34.4572 | | | 357.055 | 263.152 |
| $E$ (kcal/mole) | 16.0015 | 5.22076 | 6.91164 | 8.82037 | 34.4227 | 9.19131 | 13.0552 | 12.6338 |
| q span (°C) | | 325–800 | 325–800 | 325–800 | | 352–800 | 325–800 | 325–800 |
| $r_m$ | 0.843319 | | | | 0.911942 | | | |
| $\dot{T}$ (°C/min) | 8.23 | | | | 8.33 | | | |
| $T_m$ (°C) | 546 | | | | 605 | | | |
| $\dot{T}_m$ (°C/min) | 9.92 | | | | 9.835 | | | |
| $T_r$ (°C) | 1400 | | | | 1400 | | | |
| $w_m$ | 0.5170 | | | | 0.5550 | | | |
| $w_r$ | 0.913 | | | | 0.782 | | | |
| $-\dot{w}_{T_m}$ (°C)$^{-1}$ | −0.004120 | | | | −0.005915 | | | |

[a] $r_m$, $\bar{T}$, $T_r$, $w_r$ values under MAXRAX used for TRIM. MAXRAX $n$ used for one TRIM run; two additional $n$'s were assumed for TRIM.

The general theory revealed that large ($n$, $E$, $r_m$, $T_m$, $w_m$, $w_r$) values and small ($A$, $-\dot{w}_T$) values were consistent with high thermal stability. With the exception of the parameter $A$ for unknown reasons, this was generally the case for the graphite cloth materials. This correlation failed, however, for the carbon cloth materials. The failure was tentatively attributed to carbon cloth pyrolysis.

TABLE III

MAXRAX AND TRIM EMPIRICAL KINETIC PARAMETERS: GRAPHITE CLOTH MATERIALS[a]

| Case | *Phenol formaldehyde* | | | | *Phenylphenol phenol formaldehyde* | | | |
|---|---|---|---|---|---|---|---|---|
| | *(MAXRAX)* | *(TRIM)* | *(TRIM)* | *(TRIM)* | *(MAXRAX)* | *(TRIM)* | *(TRIM)* | *(TRIM)* |
| $n$ | 1.95836 | 1 | 1.95836 | 2 | 3.84455 | 1 | 2 | 3.84455 |
| $A$ (min$^{-1}$) | 1953.91 | 11.0609 | 932.566 | 1159.62 | $5.29334 \times 10^{13}$ | 59.7115 | 2550.76 | $1.42428 \times 10^{7}$ |
| $A'$ (min$^{-1}$) | | 20.0394 | 1020.49 | 1239.54 | | 202.175 | 6267.20 | $1.79650 \times 10^{7}$ |
| $E$ (kcal/mole) | 15.6472 | 9.00373 | 14.3326 | 14.6013 | 52.0113 | 11.9552 | 16.7266 | 28.1058 |
| q span (°C) | | 325–800 | 325–800 | 325–800 | | 381–740 | 381–740 | 381–740 |
| $r_m$ | 0.844740 | | | | 0.945849 | | | |
| $\dot{T}$ (°C/min) | 8.28 | | | | 8.28 | | | |
| $T_m$ (°C) | 516 | | | | 524 | | | |
| $\dot{T}_m$ (°C/min) | 10.00 | | | | 10.00 | | | |
| $T_r$ (°C) | 1400 | | | | 1400 | | | |
| $w_m$ | 0.5730 | | | | 0.6550 | | | |
| $w_r$ | 0.843 | | | | 0.884 | | | |
| $-\dot{w}_{T_m}$ (°C)$^{-1}$ | −0.003695 | | | | −0.007010 | | | |

| Case | *Polyphenylene* | | | | *Polyimide* | | | |
|---|---|---|---|---|---|---|---|---|
| | *(MAXRAX)* | *(TRIM)* | *(TRIM)* | *(TRIM)* | *(MAXRAX)* | *(TRIM)* | *(TRIM)* | *(TRIM)* |
| $n$ | 2.02777 | 1 | 2 | 2.02777 | 1.00000 | 1.00000 | 2 | 3 |
| $A$ (min$^{-1}$) | 8247.30 | 16.4820 | 915.500 | 1049.00 | 21207.6 | 70.2077 | 3766.01 | 435416 |
| $A'$ (min$^{-1}$) | | $5.27640 \times 10^{21}$ | 1043.41 | 1167.27 | | 212.102 | 10262.3 | 996153 |
| $E$ (kcal/mole) | 17.7322 | 9.43783 | 14.2131 | 14.3649 | 21.4858 | 12.7503 | 18.1404 | 24.7624 |
| q span (°C) | | 325–740 | 325–740 | 325–740 | | 419–774 | 419–774 | 419–774 |
| $r_m$ | 0.860132 | | | | 0.868221 | | | |
| $\dot{T}$ (°C/min) | 8.23 | | | | 8.28 | | | |
| $T_m$ (°C) | 517 | | | | 617 | | | |
| $\dot{T}_m$ (°C/min) | 9.94 | | | | 11.54 | | | |
| $T_r$ (°C) | 1400 | | | | 1400 | | | |
| $w_m$ | 0.5730 | | | | 0.4348 | | | |
| $w_r$ | 0.850 | | | | 0.885 | | | |
| $-\dot{w}_{T_m}$ (°C)$^{-1}$ | −0.00404 | | | | −0.00593 | | | |

---

[a] $r_m$, $\dot{T}$, $T_r$, $w_r$ values under MAXRAX used for TRIM. MAXRAX $n$ used for one TRIM run; two additional $n$'s were assumed for TRIM.

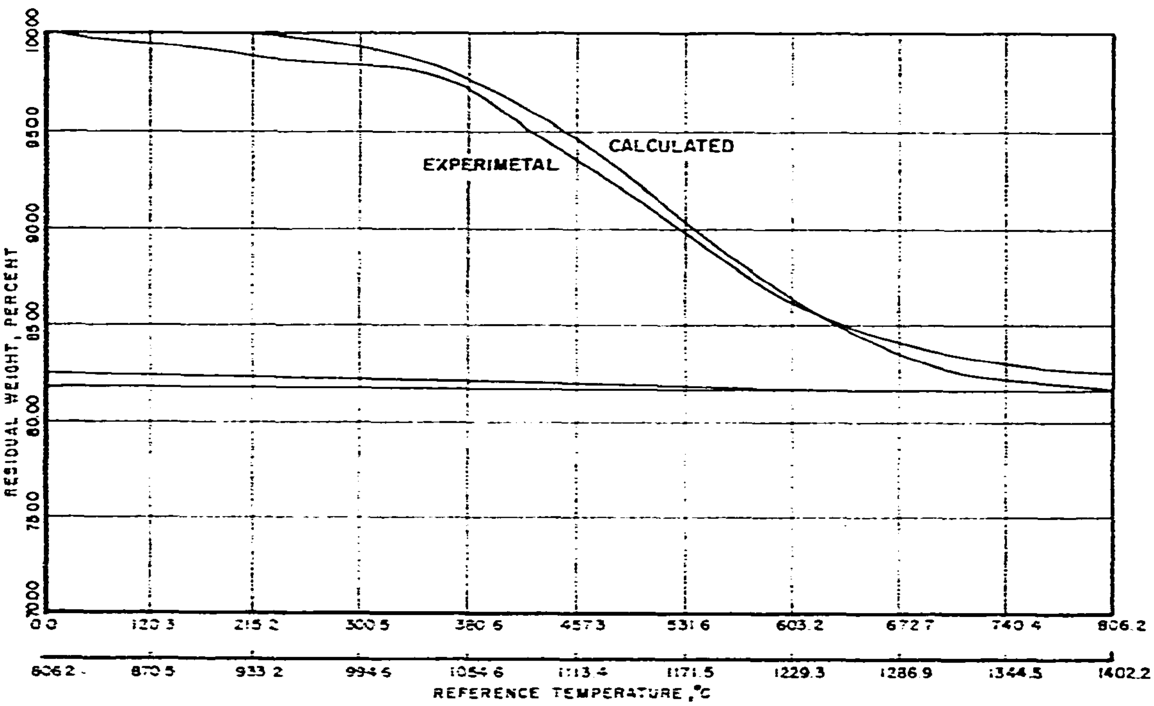

Fig. 8. Calculated and experimental curves for the phenol formaldehyde–carbon cloth material.

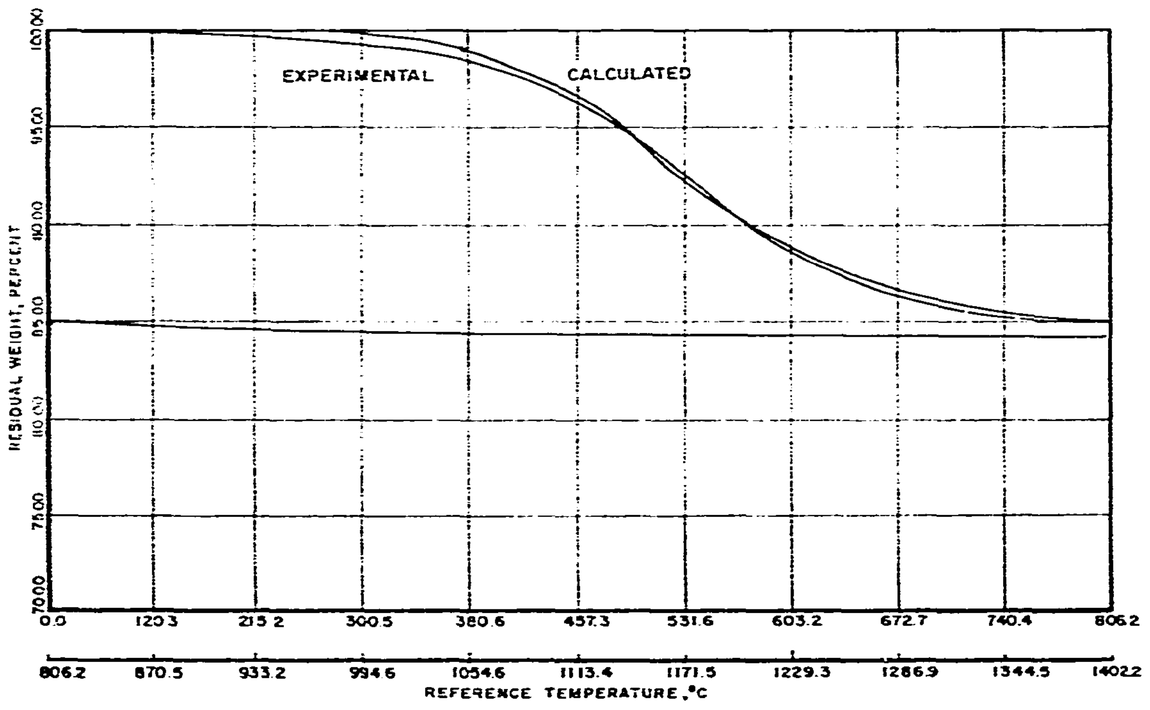

Fig. 9. Calculated and experimental curves for the phenol formaldehyde–graphite cloth material.

MAXRAX–PAR 3 curves were compared with the experimental ones. As shown by Figs. 8 and 9, the typical trend was to over-predict the experimental curve below the maximum rate point and under-predict low weights at higher temperatures. The error was, on the average, about evenly divided between the two regions. The best agreement was near the maximum rate point.

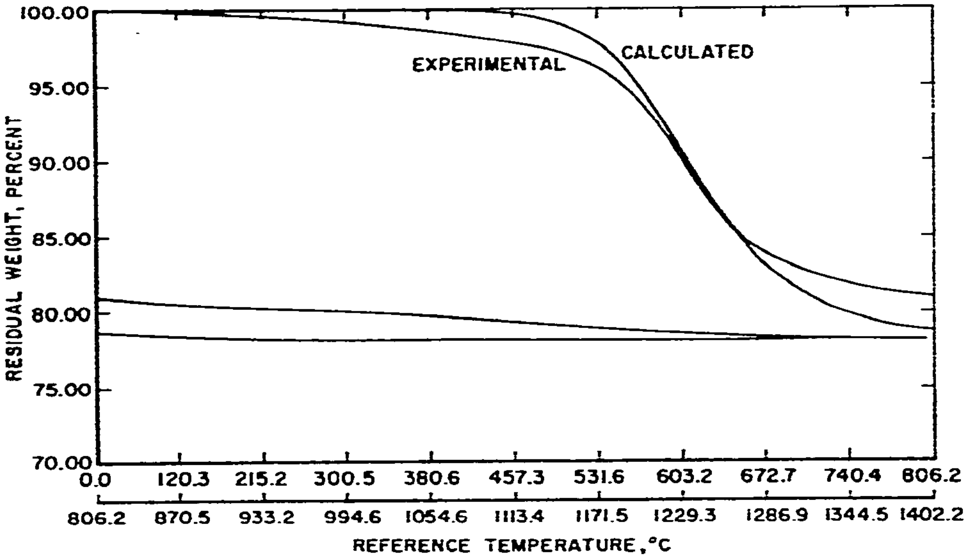

Fig. 10. Calculated and experimental curves for the polyimide–carbon cloth material.

The maximum calculated–experimental weight difference at constant temperature ranged from about 0.8% for phenol formaldehyde–graphite cloth (Fig. 9) up to 2.3% for polyimide–carbon cloth (Fig. 10). Table IV summarizes weight differences for composites as a function of temperature.

A subjective evaluation of overall MAXRAX curve-fitting for the graphite cloth materials was phenol formaldehyde > phenylphenol phenol formaldehyde > polyphenylene > polyimide. The ranking was polyphenylene > phenol formaldehyde > polyimide > polybenzimidazole for the carbon cloth materials. The graphite cloth materials were clearly fitted better than the carbon cloth cases.

The phenol formaldehyde–carbon cloth material underwent high weight loss at low temperature and a binary pyrolysis mechanism (see Fig. 8). MAXRAX was applied to three cases: step 1 ending at 480°C, step 2 from 480°C to 1400°C, and an average case using step 2 data. The PAR 3 curves for two separate steps did not fit smoothly. Although not necessarily correct from a physicochemical viewpoint, the average set gave the best empirical fit (see Table II).

A multiple-step pyrolysis was also found for polybenzimidazole–carbon cloth. Three MAXRAX cases were run: step 1 ending at 457°C, step 2 from 457°C to 1400°C, and an average using step 2 data. Even though the PAR 3 curves for the binary mechanism were found to fit smoothly, the average set was still felt to best represent

TABLE IV

CALCULATED AND EXPERIMENTAL WEIGHT FRACTIONS

| *Case* | *300°C* | | *500°C* | | *800°C* | | *1000°C* | | *1400°C* | |
|---|---|---|---|---|---|---|---|---|---|---|
| | $w_0$ | $(w_{00} - w_0)$ | $w_0$ | $(w_{00} - w_0)$ | $w_0$ | $(w_{00} - w_0)$ | $w_0$ | $(w_{00} - w_0)$ | $w_0$ | $(w_{00} - w_0)$ |
| Carbon cloth | | | | | | | | | | |
| Phenol Formaldehyde | 0.984 | 0.009 | 0.914 | 0.008 | 0.826 | −0.008 | 0.823 | 0.006 | 0.816 | −0.003 |
| Polybenzimidazole | 0.982 | 0.018 | 0.975 | 0.015 | 0.925 | −0.003 | 0.910 | −0.020 | 0.883 | −0.003 |
| Polyphenylene | 0.989 | 0.011 | 0.971 | 0.004 | 0.922 | −0.007 | 0.917 | 0.005 | 0.913 | 0.000 |
| Polyimide | 0.992 | 0.008 | 0.971 | 0.019 | 0.811 | −0.023 | 0.800 | −0.018 | 0.782 | 0.000 |
| Graphite cloth | | | | | | | | | | |
| Phenol Formaldehyde | 0.994 | 0.004 | 0.942 | 0.000 | 0.848 | 0.002 | 0.845 | 0.000 | 0.843 | 0.000 |
| Phenylphenol Formaldehyde | 0.996 | 0.004 | 0.974 | 0.004 | 0.897 | −0.009 | 0.876 | 0.000 | 0.884 | 0.001 |
| Polyphenylene | 0.995 | 0.004 | 0.941 | 0.002 | 0.856 | 0.000 | 0.853 | −0.003 | 0.850 | 0.000 |
| Polyimide | 0.996 | 0.004 | 0.985 | 0.003 | 0.900 | −0.005 | 0.893 | −0.008 | 0.885 | 0.000 |

the experimental curve (Table II). Other visually suggested steps could not be practically resolved with a straight edge (see Fig. 3).

TRIM was a computer code for the computation of kinetic parameters from experimental weight fractions as a function of temperature. Up to 99 data points to 806°C were possible with 67 (325°C–800°C) being used in most cases. One TRIM $n$ value was taken from MAXRAX. Two additional integers covering the nominal $n$ span of unity to three were also run.

The nominal TRIM ranges for the carbon cloth materials were $n = 1$–$3$, $A = 6.4 \times 10^{-1}$–$6.3 \times 10^{7}$, $E = 5.2$–$13$. The ranges for the graphite cloth materials were $n = 1$–$3.8$, $A = 1.1 \times 10^{1}$–$1.4 \times 10^{7}$, $E = 9$–$28$.

The parameter $n$ influenced both $A$ and $E$. Polyimide–carbon cloth $n$ values of 1 and 2 gave the minimum effect with $A = 6$, 106 and $E = 9$, 13, respectively. For polyphenylene–graphite cloth, $n = 1, 3.8$ gave $A = 6.0 \times 10^{1}$, $1.4 \times 10^{7}$, and $E = 12, 28$, the worst case. An increase in $n$ gave a corresponding increase in $A$ and $E$ with the single exception of polyimide–carbon cloth. An increase in $n$ also gave an apparent less stable material (due to $A$ and $E$ increase).

TRIM–PAR 3 curves were prepared for comparison with the experimental one. The trend for TRIM was to predict slightly better agreement than MAXRAX at the beginning and end of the curve. MAXRAX generally gave the best agreement within the maximum rate of weight loss region. Fig. 11 illustrates these trends.

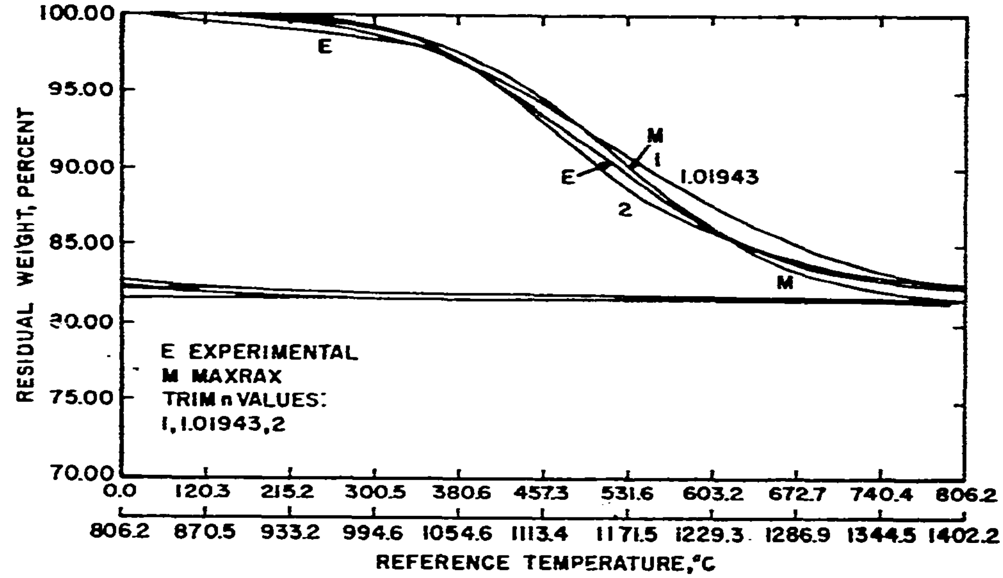

Fig. 11. Calculated (using TRIM and MAXRAX) and experimental curves for the phenol formaldehyde–graphite cloth material.

The maximum TRIM–PAR 3 calculated *vs.* experimental weight difference at constant temperature ranged from about 0.8% for phenylphenol phenol formaldehyde–graphite cloth to 4% for polyimide–carbon cloth.

TRIM–PAR 3 curves were very similar to the MAXRAX–PAR 3 curves for the case of the *n* integer closest to the MAXRAX value. On this basis, the overall curve-fitting of TRIM, in terms of specific material, was only slightly different from that of MAXRAX.

*A'* was a check for the TRIM method of least squares. This hybrid parameter used both maximum rate data and the TRIM value of *E*. The TRIM values of *A* and *A'* usually agreed within factors of 2–3 (excluding phenylphenol phenol formaldehyde–graphite cloth). The fact that the largest MAXRAX and TRIM curves differences were in the maximum rate region suggested that a factor of three variation between *A* and *A'* was not unreasonable.

The interrelations between *n*, *A*, and *E* were examined by a PAR 3 parametric study. A $\dot{T}$ of 8°C/min was used with a $w_r$ of 0.55. The 32 cases revealed that an increase in either *n* or *E*, or a decrease in *A*, gave a more stable curve, as suggested by theory. In addition, virtual sets of (*n*, *A*, *E*) were found to closely approximate a single curve. Fig. 12 illustrated well typical intersections of pairs of curves.

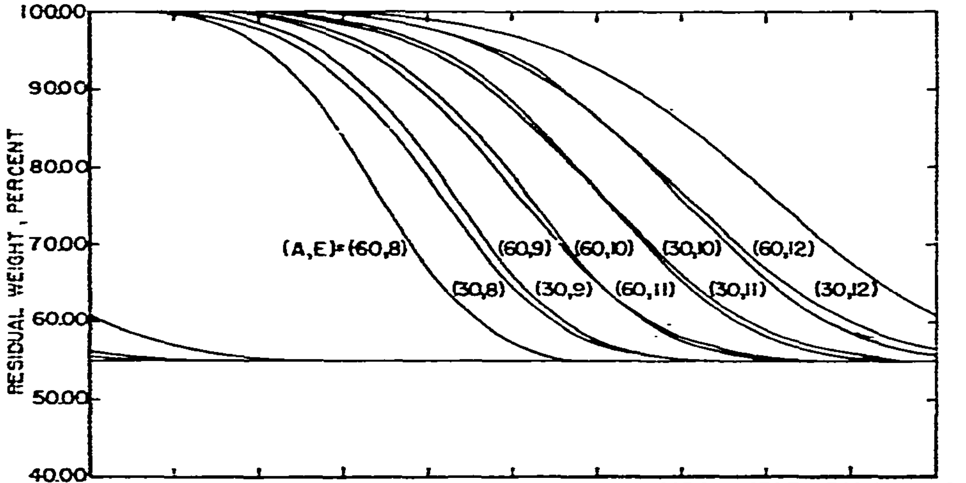

Fig. 12. Study of the interrelationships between the empirical kinetics parameters *n*, *A*, and *E*.

There is a possible erroneous evaluation of virtual sets of parameters if experimental and analysis errors are large.

## CONCLUSIONS

The range of thermal stability was large for representative aromatic and heterocyclic polymers.

· The highest stability was found for a polybenzimidazole and then two polyimide heterocyclics. The decreasing order for the aromatics was for two polyphenylenes and then three phenol formaldehydes.

The overall TG of the cloth reinforced polymers was represented by rate parameters for an Arrhenius type correlation.